Journal of Energy and Power Engineering 12 (2018) 44-56
doi: 10.17265/1934-8975/2018.01.006

Characterization of Photovoltaic Modules under Arid Environments

Abubaker Younis [1, 2], Yousef Alhorr[1], Esam Elsarrag [1] and Mahmoud Onsa[2]

1. Gulf Organization for Research and Development, Qatar Science and Technology Park, Tech 1 Level 2, 203, Qatar (email: a.younis@gord.qa, e.elsarrag@gord.qa)

2. Department of Mechanical Engineering, Faculty of Engineering, University of Khartoum, Khartoum, Sudan (email:onsa@uofk.edu)

Abstract: The performance of solar photovoltaic (PV) cell/module under extreme ambient temperatures and insolations was utilized to help to present a simplified PV power characterization method for the particular case of the arid environment. Validation of the introduced modeling technique was done by comparing data produced by the numerical simulation with those obtained by laboratory and outdoor tests conducted on crystalline silicon technology modules. Performance curves and bar chart of power production demonstrated the validation results of the different experiments, which in turn proved the existence of an acceptable error margin.

Key words: Photovoltaics, electrical characteristics, single-diode model, MATLAB.

1. Introduction

A solar photovoltaic (PV) cell/module has always been defined as the semiconductor device that converts sunlight into electricity [1]. The modeling and simulation of those devices' electrical behavior is a standard practice that the scientific community widely reported it. In reported literature, various approaches have been employed to express the electrical behavior of solar cell/module. Rauschenbach [2], Townsend [3], Eckstein [4], and Schroder [5] reviewed several models and their utility for system design purposes. The single diode model, in particular, was studied intensively among authors. Azzouzi et al. [6] work was focused on the single-diode model, in which I-V and P-V characteristics were functions of series resistance, parallel resistance, cell temperature, and solar irradiation. Bikaneria et al. [7] also introduced the same characterization model, its theory, and construction.

Corresponding author: Esam Elsarrag, Ph.D., professor, research fields: building and energy, renewable energy, built environment. Email: elsarrag@hotmail.com.

The effect of the surrounding environment on the solar PV systems was researched during its operation in several respects. Muralidharan [8] analyzed the effect of changing physical and environmental factors on the I-V characteristics of a solar PV cell. Ghosh et al. [9] defined a circuit-based simulation model for a PV module to find its electrical characteristics during ambient temperature and solar irradiation change.

The application of simulation, especially using the software in this, was an exciting PV power research topic addressed by researchers. Elias et al. [10] simulated an ideal solar PV cell using Matlab software. The process was carried out to evaluate the influence of the variation in solar cell temperature, solar irradiation, diode ideality factor, and energy gap on the I-V and P-V characteristics of the solar cell. Petkov et al. [11] used the standard and modified versions of the single-diode model to simulate the electrical behavior of solar PV cells by using Mathcad software. Anku et al. [12] also followed the same software-based approach, besides introducing an optimization technique that uses blocks from the Matlab /Simulink library to ensure efficient use of PV modules, besides

introducing an optimization technique to ensure efficient use of PV modules using blocks from the Matlab /Simulink library. Patel and Sharma [13] and Fares et al. [14] also depended on Matlab/Simulink software for modeling, simulation, and implementation of the solar cell models. The obtained characteristics represented both single-cell and complete PV module.

In recent years, substantial progress has been made in the development of mathematical models to sufficiently describe the electrical system of PV modules. However, for the accurate prediction of the electrical behavior of PV modules, a comprehensive and precise model is of interest thus far. Notably, the model could be used by engineers in a variety of climates. This article presents a model and a solution algorithm, which can be used to characterize the performance of a PV cell\module under extreme environmental conditions of solar irradiation and ambient temperature. The introduced approach was validated against experimentally obtained data.

2. Experimental Setup and Procedure

2.1 Indoor Arrangement

The trials took place inside an Atlas SEC 1100 weather simulation chamber, which has a size of 1100 liters with an active radiation area of $5{,}600\ cm^2$. The chamber acts as a perfect test environment for small to medium-sized PV panels. The integrated Metal Halide Global lamp (MHG Model: 4000 W Luminary) conforms with IEC 60904 Class A guidelines and provides a quality solar simulation that has a close spectral match to the natural sunlight plus high irradiation efficiency and spatial uniformity in the test area. The MHG lamp provides adjustable output up to a maximum of $1{,}200\ W/m^2$ with a spectral range of $280 - 3{,}000\ nm$. The controlled parameters by the chamber include air (ambient) temperature, solar irradiation, and relative humidity via a touch screen control panel located on the front of the chamber. The weather apparatus can log data from a six-channel DAQ, which in turn can connect temperature sensors, solar irradiation pyranometer, and black standard temperature control, all in real-time.

A 50 W mono-crystalline solar PV unit, RNG-50D manufactured by Renogy, was used. Fig. 1 shows the PV panel placed inside the chamber. The tests monitored the response of Renogy's module at two solar irradiation levels: $700\ W/m^2$, and $1{,}200\ W/m^2$, while The humidity was kept constant at 30%. For each level, the chamber temperature was repeatedly changed to obtain different temperature measurements of the PV module. Data were recorded for the open-circuit voltage, the short circuit current, the voltage, and the current of the solar PV module at changing resistance load starts from 1 Ohm and up to 100 Ohm.

A 50 W load was connected to the solar PV module. The load was built from number of 1 Ohm, 4 Ohm and 8 Ohm resistors connected in series via a custom-made micro-controller based relay network to achieve different progressive resistive values from 1 to 100 Ohm by a step size of 1 Ohm. The electrical output of the solar PV unit keeps its consistency by setting each resistance level for 5 minutes under the same conditions. Although the upper resistance limit was set to 100 Ohm, the maximum possible resistance would never go above a dozen or so Ohms in practice. The module power was measured by a separate microcontroller based system linked to the load and used an ACS712ELECTR-05B-T based current sensor and voltage divider coupled with 10bit ADC of the micro board, which provided resolutions of 0.009 A and 0.005 V for the current and voltage, respectively.

The temperature of the solar PV module was measured at six different points of its backside by Class B PT100 temperature sensors to obtain an average value. The solar irradiation at the plane of the PV panel was measured using an ISO 9060 first class-compliant Kipp & Zonen CMP 6 pyranometer (inside the SEC) which can measure up to $2{,}000\ W/m^2$ in a spectral range of 285 to 2,800 nanometers with a sensitivity of 12.29 x 10-6 μV/Wm^{-2} and a 180 °field of view. Fig. 2 displays a sketch of the full test setup.

Fig. 1 On the right, a pictorial illustration of the solar panel inside the SEC 1100 chamber. On the left, the back of the solar panel and the temperature sensors fixed on it.

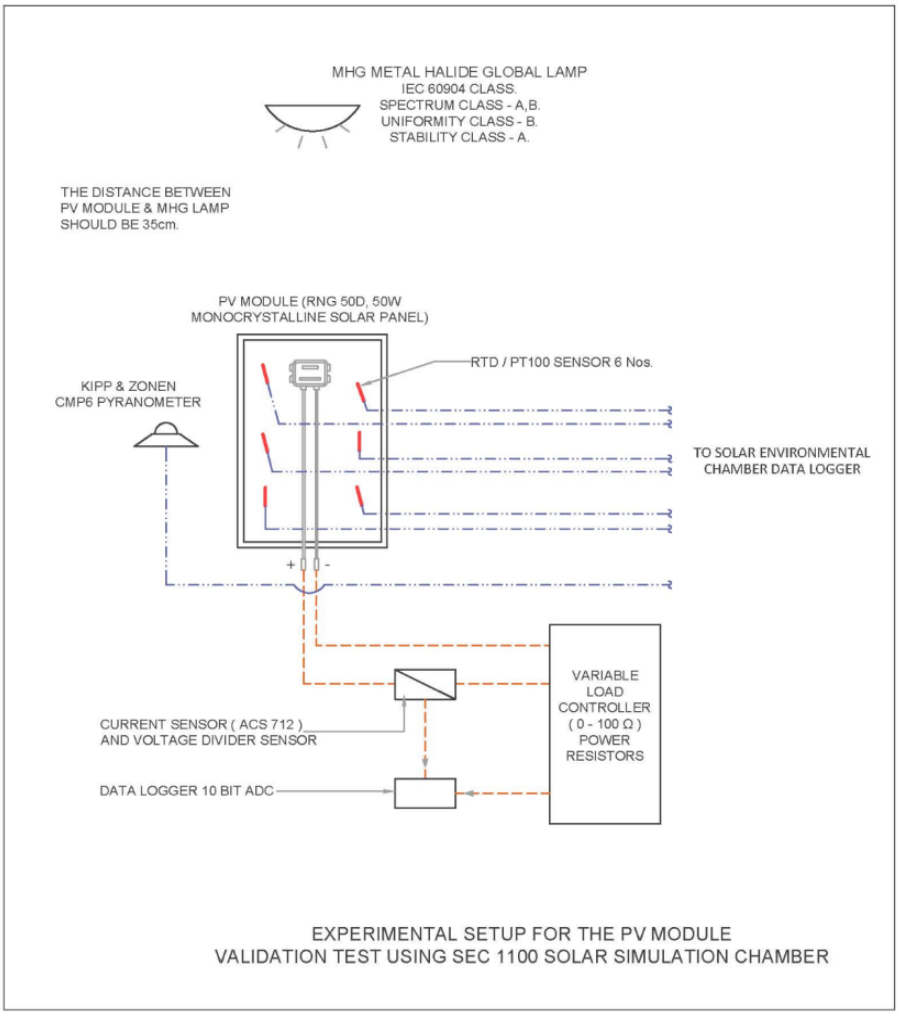

Fig. 2 Sketch of the test setup for the monocrystalline silicon PV module.

2.2 Outdoor Arrangement

A set of four 250 W polycrystalline solar PV modules was mounted in the open, to produce again data that can be used to verify the proposed model and its solution sequence. Fig. 5 depicts the arrangement used for the outdoor experiments. Monitoring and logging of the electrical characteristics of the solar PV set was done automatically by a custom-made

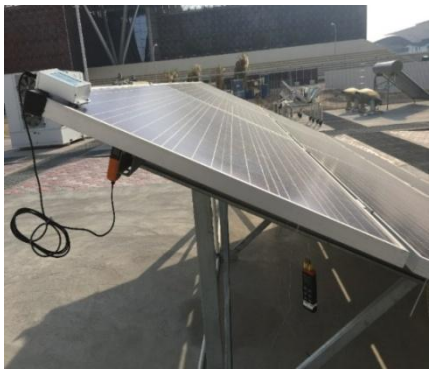

Fig. 3 Photographic view of the outdoor setup of the polycrystalline PV set.

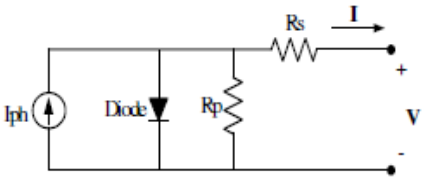

Fig. 4 The solar PV cell equivalent circuit of the single diode model.

microcontroller-based smart data logging system, which measures every parameter with different sensors. The current was measured using ACS712 based current sensors, which can measure DC in both directions with a range of 20 Amps, and an accuracy of 1.5%. The weather data for the year of 2017 was collected using Vantage Pro 2 weather station model manufactured by Davis® weather monitoring.

3. Modeling and Solution Algorithm

Fig. 1 shows the equivalent electrical circuit of a solar PV cell according to the single diode model [15]. The circuit consists of photocurrent source, diode, shunt or parallel resistor, and series resistor in the load branch.

The current and voltage (I-V) characteristics of the single diode model-derived utilizing Kirchhoff law- is given by [16]:

$$I = I_{ph} - I_d - I_p = I_{ph} - I_o \times \left[e^{\left(\frac{V+I\times R_s}{A\times N_s\times v_T}\right)} - 1 \right] - \frac{V + I \times R_s}{R_p} \quad (1)$$

Where light or photocurrent (I_{ph}), diode reverse saturation current (I_o), and shunt or parallel resistance (R_p) are the unknowns. The equation corresponding to each of the three parameters is a function of cell temperature and solar irradiation.

I_{ph} is a function of solar irradiation (G), cell temperature (T_c), and temperature coefficient of short circuit current (μ_{sc}). Its governing equation under any operational condition is given by [17]:

$$I_{ph} = \frac{G}{G_{ref}} \times \left[I_{ph,ref} + \mu_{sc} \times \Delta T \right] \quad (2)$$

Where,

G_{ref} is reference value of solar irradiation and equals to $1000 \frac{W}{m^2}$

$I_{ph,ref}$ is the photocurrent at reference conditions (Standard Testing Conditions (STC)), and it can be approximated to [17]:

$$I_{ph,ref} = I_{sc,ref} \quad (3)$$

Where $I_{sc,ref}$ is the reference value of the solar PV module short circuit current.

ΔT is a temperature difference, which is given by $\Delta T = T_c - T_{c,ref}$, where $T_{c,ref} = 298K$ is the reference temperature.

The well-known I_o equation is given by [16]:

$$I_o = D \times {T_c}^3 \times e^{\left(\frac{-q\times\varepsilon_G}{A\times N_s\times \mathrm{K}\times T_c}\right)} \quad (4)$$

Where D is the diode diffusion factor, and ε_G is the material bandgap energy, which equals 1.11 eV for silicon at 300 K [18].

Dividing the two sides in Eq. (4) by I_o at STC conditions, the result is:

$$I_o = I_{o,ref} \times \left(\frac{T_C}{T_{c,ref}}\right)^3 \times e^{\left[\left(\frac{q\times\varepsilon_G}{A\times N_s\times K}\right)\times\left(\frac{1}{T_{c,ref}} - \frac{1}{T_c}\right)\right]} \quad (5)$$

Diode reverse saturation current at STC ($I_{o,ref}$) is approximated by [19]:

$$I_{o,ref} = I_{sc,ref} \times e^{\left(\frac{-V_{oc,ref}}{A\times N_s\times v_T}\right)} \quad (6)$$

Merging Eq. (6) into Eq. (5) results in:

$$I_o = I_{sc,ref} \times \left(\frac{T_C}{T_{c,ref}}\right)^3 \times e^{\left(\frac{-V_{oc,ref}}{A\times N_s\times v_T}\right)} \times e^{\left[\left(\frac{q\times\varepsilon_G}{A\times N_s\times K}\right)\times\left(\frac{1}{T_{c,ref}} - \frac{1}{T_c}\right)\right]} \quad (7)$$

Where, A is the ideality factor, which depends on the PV technology. A values are 1.2 and 1.3 for mono and polycrystalline silicon, respectively [20].

N_s is the number of cells connected in series,

v_T is the thermal voltage and is given by:

$$v_T = \frac{k \times T_c}{q} \tag{8}$$

Where,

k is Boltzmann's constant $\left(1.381 \times \frac{10^{-23} J}{K}\right)$

q is the electronic charge $(1.602 \times 10^{-19} coulomb)$

T_c is the solar cell temperature.

Ahmad et al. [19] stipulated in the chosen value of R_p when substituted in Eq. (1) to make the computed maximum power equals the maximum experimental power at the reference conditions point. Consequently, Eq. (1) becomes:

$$I_{mp,ref} = I_{ph,ref} - I_{o,ref} \times \left[e^{\left(\frac{V_{mp,ref}+I_{mp,ref}\times R_s}{A\times N_s\times v_T}\right)} - 1\right] - \frac{V_{mp,ref} + R_s \times I_{mp,ref}}{R_p} \tag{9}$$

Therefore R_p is:

$$R_p = \frac{V_{mp,ref} + R_s \times I_{mp,ref}}{I_{sc,ref} - I_{sc,ref} \times e^{\left(\frac{V_{mp,ref}+I_{mp,ref}\times R_s - V_{oc,ref}}{A\times N_s\times v_T}\right)} + I_{sc,ref} \times e^{\left(\frac{-V_{oc,ref}}{A\times N_s\times v_T}\right)} - \frac{P_{max,ref}}{V_{mp,ref}}} \tag{10}$$

The effect of temperature on open-circuit voltage, short circuit current, and maximum power of the solar PV cell is given by:

$$V_{oc} = V_{oc,ref} \times \left(1 - \mu_{oc} \times \left(T_c - T_{c,ref}\right)\right) \tag{11}$$

$$I_{sc} = I_{sc,ref} \times \left(1 + \mu_{sc} \times \left(T_c - T_{c,ref}\right)\right) \tag{12}$$

$$P_{max} = P_{max,ref} \times \left(1 - \mu_{mp} \times \left(T_c - T_{c,ref}\right)\right) \tag{13}$$

Updating Eq. (7), and Eq. (10) by Eqs. (11)-(13):

$$I_o = I_{sc} \times \left(\frac{T_C}{T_{c,ref}}\right)^3 \times e^{\left(\frac{-V_{oc}}{A\times N_s\times v_T}\right)} \times e^{\left[\left(\frac{q\times \varepsilon_G}{A\times N_s\times \mathrm{K}}\right)\times\left(\frac{1}{T_{c,ref}} - \frac{1}{T_c}\right)\right]} \tag{14}$$

$$R_p = \frac{V_{mp,ref} + R_s \times I_{mp,ref}}{I_{sc} - I_{sc} \times e^{\left(\frac{V_{mp,ref}+I_{mp,ref}\times R_s - V_{oc}}{A\times N_s\times v_T}\right)} + I_{sc} \times e^{\left(\frac{-V_{oc}}{A\times N_s\times v_T}\right)} - \frac{P_{max}}{V_{mp,ref}}} \tag{15}$$

The variation in the voltage of experiments made it possible to describe it by the natural logarithmic function approximately. Therefore, the voltage generating function of time (t) is given by:

$$V = lnt \tag{16}$$

For simplification purposes, the series resistance (R_s) is neglected. It is also due to the relatively small magnitudes of R_s when compared to R_p .

Löper et al. [21] suggested to add a constant offset to V_{oc} as a fit parameter to have a numerical solution converges to data of the experiments. Adding $V_{oc,ref}$ as an offset to Eq. (11), the result becomes:

$$V_{oc}{}^* = V_{oc,ref} \times \left(1 + \mu_{oc} \times \left(T_c - T_{c,ref}\right)\right) \tag{11}^*$$

Updating Eq. (14), and Eq. (15) by Eq.(11)*, the new statement of I_o will be:

$$I_o = I_{sc} \times \left(\frac{T_C}{T_{c,ref}}\right)^3 \times e^{\left(\frac{-V_{oc}{}^*}{A\times N_s\times v_T}\right)} \times e^{\left[\left(\frac{q\times \varepsilon_G}{A\times N_s\times \mathrm{K}}\right)\times\left(\frac{1}{T_{c,ref}} - \frac{1}{T_c}\right)\right]} \tag{14}^*$$

And for the resistance in parallel:

$$R_p = \frac{V_{mp,ref} + R_s \times I_{mp,ref}}{I_{sc} - I_{sc} \times e^{\left(\frac{V_{mp,ref} + I_{mp,ref} \times R_s - V_{oc}^*}{A \times N_s \times v_T}\right)} + I_{sc} \times e^{\left(\frac{-V_{oc}^*}{A \times N_s \times v_T}\right)} - \frac{P_{max}}{V_{mp,ref}}} \quad (15)^*$$

Table 1 Renogy's RNG-50D PV module electrical and thermal properties.

Electrical Data	
Maximum power at STC	50 W
Optimum operating voltage (V_{mp})	18.5 V
Optimum operating current (I_{mp})	2.7 A
Open circuit voltage (V_{oc})	22.7 V
Short circuit current (I_{sc})	2.84 A
Module efficiency	14.67%
Thermal characteristics	
Operating module temperature	-40 to $+90$℃
Nominal operating cell temperature (NOCT)	47 ± 2℃
Temperature coefficient of P_{max} (μ_{mp})	$-0.23\,\%/^\circ C$
Temperature coefficient of V_{oc} (μ_{oc})	$-0.33\,\%/$℃
Temperature coefficient of I_{sc} (μ_{sc})	$0.05\,\%/$℃
Number of cells	36 (4 x 9)
Solar cell type	Monocrystalline

Table 2 Solarturk energi STR60 PV module electrical and thermal properties.

Electrical Data	
Maximum power at STC	250 W
Optimum operating voltage (V_{mp})	29.98 V
Optimum operating current (I_{mp})	8.34 A
Open circuit voltage (V_{oc})	37.41 V
Short circuit current (I_{sc})	8.79 A
Module efficiency	15.3%
Thermal characteristics	
Operating module temperature	-40 to $+120$℃
Nominal operating cell temperature (NOCT)	47 ± 2℃
Temperature coefficient of P_{max} (μ_{mp})	$-0.43\,\%/$℃
Temperature coefficient of V_{oc} (μ_{oc})	$-0.32\,\%/$℃
Temperature coefficient of I_{sc} (μ_{sc})	$0.05\,\%/$℃
Number of cells	60 (6 x 10)
Solar cell type	Polycrystalline

All values for the electrical and thermal properties of solar cells included in the above equations are listed in Table 1 and Table 2.

4. Results and Discussions

The numerical solution of the implicit nonlinear I-V characteristics equation, which is presented by Eq. (1), is of interest to evaluate the current and voltage that is produced by the PV cell. Fzero command, which is provided by Matlab software, is a solver that combines the bisection, secant, and inverse quadratic interpolation methods. The solution algorithm for Eq. (1) is translated into Matlab script, which necessarily contains the Fzero command. The final results are presented in the form of curves. Fig. 2 illustrates the solution algorithm flow chart.

4.1 Validation by Laboratory Data

The process of validating the numerically-generated I-V properties against those produced by indoor tests is visualized in Figs. 6 and 7 at different PV module temperature and solar irradiation. Figs. 8 and 9 show comparable P-V curves for simulation and validation. In the pre-and-post maxima region, the curves are almost identical, while a non-drastic displacement between them at the maxima region is present. Figs. 10 and 11 present the P-V performance curves generated by the numerical solution for a wide range of the PV module temperature. The curves maintain the typical P-V behavior of the solar PV cell, while the effect of temperature is dominant, and that is explicitly stated in the earlier set of governing mathematical equations. In Figs. 12 and 13, it is distinctly presented that the temperature has almost no effect on the short circuit current, which perfectly matches the PV cell theory.

4.2 Validation by Outdoor Data

The outdoor setup data were collected for the year 2017. These data facilitated testing the real-life applicability of the results presented in the previous subsection. Fig. 14 shows a bar chart of the monthly accumulation of power produced by the PV set against those simulated by the software. Fig. 15 shows a histogram of predicted versus annual performance recorded for the solar PV set. The observed difference in results between reality and simulation falls within 8%.

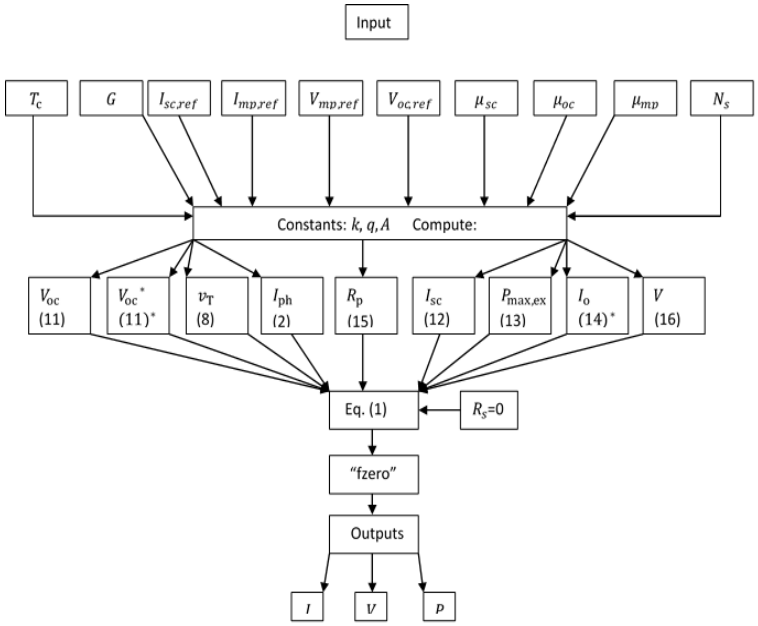

Fig. 5 The software flow chart in determining the electrical characteristics of the single diode model using the described solution algorithm (or sequence).

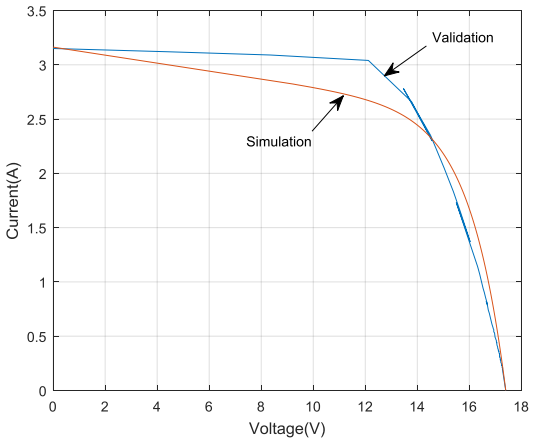

Fig. 6 Current Vs. Voltage at 66 ℃ and 900 $^{W}/_{m^2}$.

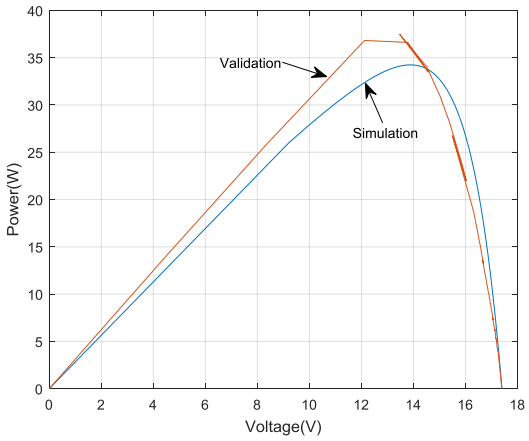

Fig. 8 Power Vs. Voltage at 95 ℃ and 1100 $^{W}/_{m^2}$.

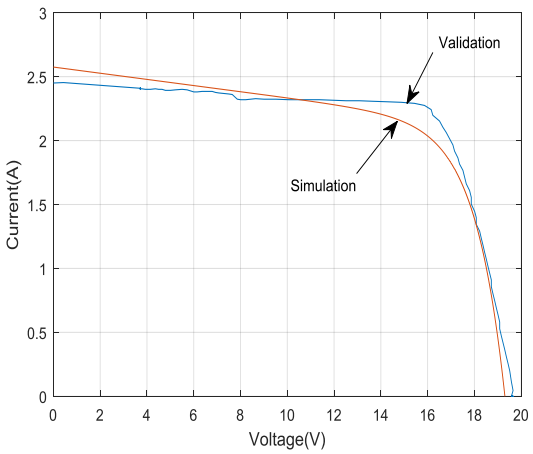

Fig. 7 Current Vs. Voltage at 95 ℃ and 1,100 $^{W}/_{m^2}$.

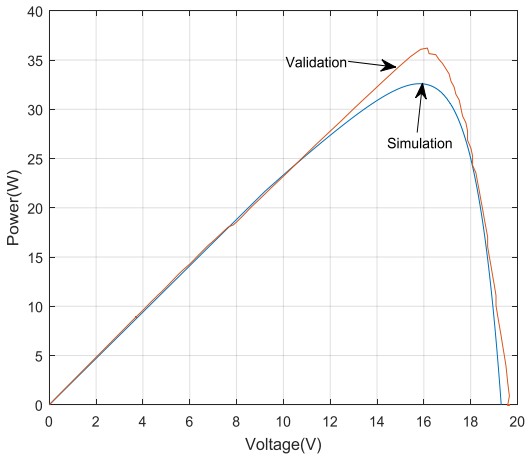

Fig. 9 Power Vs. Voltage at 66 ℃ and 900 $^{W}/_{m^2}$.

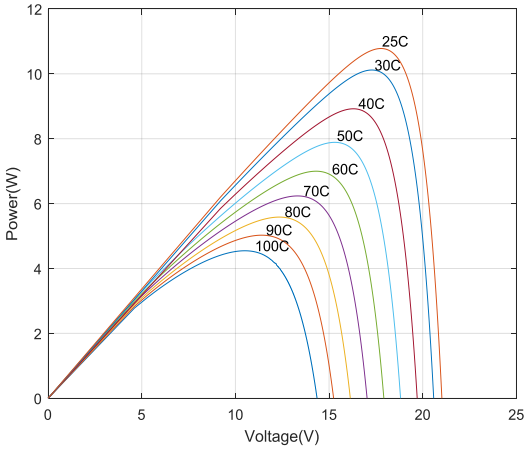

Fig. 10 Power Vs. Voltage at different temperatures and 1,000 $^{W}/_{m^2}$.

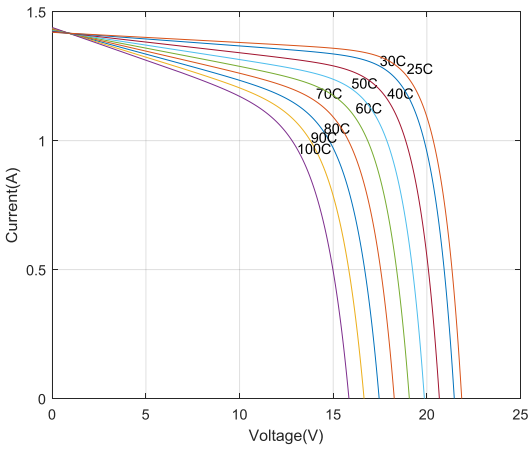

Fig. 12 Current Vs. Voltage at different temperatures and 1,000 $^{W}/_{m^2}$.

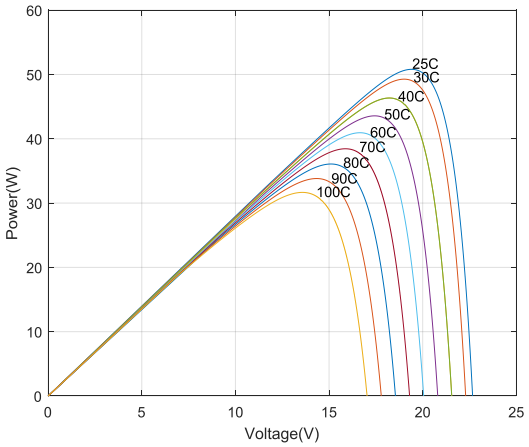

Fig. 11 Power Vs. Voltage at different temperatures and 250 $^{W}/_{m^2}$.

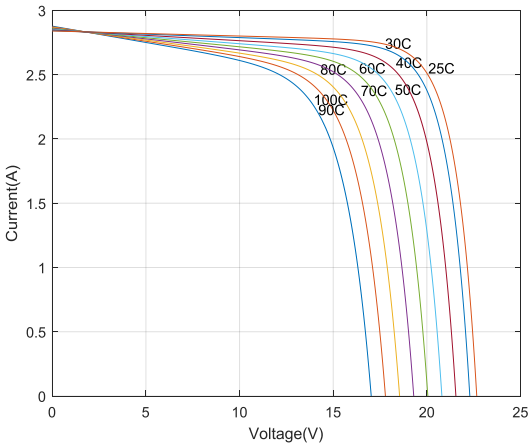

Fig. 13 Current Vs. Voltage at different temperatures and 250 $^{W}/_{m^2}$.

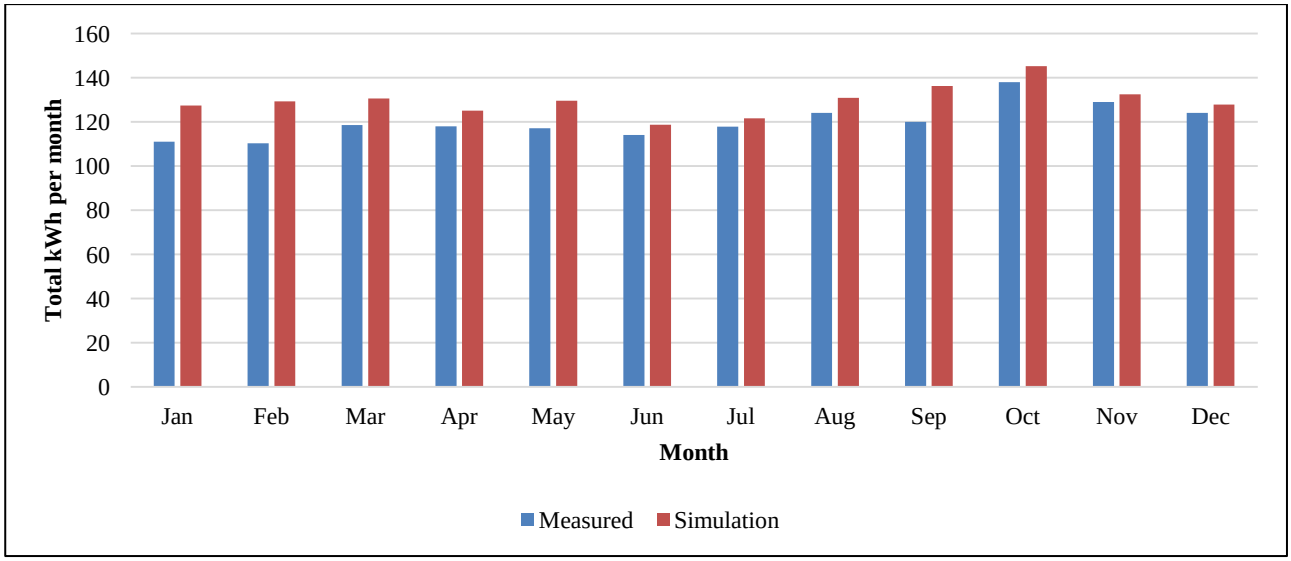

Fig. 14 Monthly accumulation of power produced by the polycrystalline silicon PV set against those simulated by the software for the year 2017.

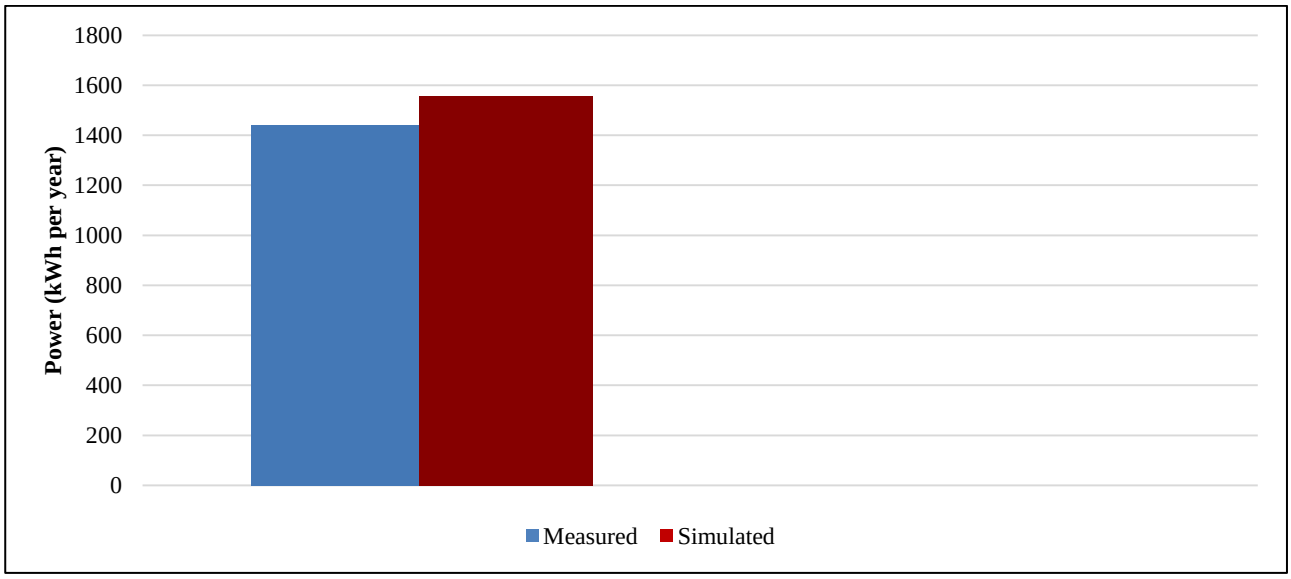

Fig. 15 Simulated versus annual power recorded for the polycrystalline silicon PV set for the year 2017.

5. Conclusions

A solution algorithm was introduced for the relatively modified single diode model, which depends, in its implementation, on the Matlab software. The results obtained in the form of I-V and P-V curves illustrate the difference between the indoor and outdoor experimental data and those numerically generated. Also, it is noticeable a somewhat match between these curves. The presented convergence in performance is acceptable for non-delicate applications of PV systems. The annual-wise power production prediction capability of the modeling method was also illustrated in the corresponding graphs, by error margin of 8%.

Reference

[1] "Solar Photovoltaic Technology Basics | NREL." Accessed May 19, 2018. https://www.nrel.gov/workingwithus/re-photovoltaics.html.

[2] Rauschenbach, S. 1980. Solar Cell Array Design Handbook—The Principle Technology of Photovoltaic Energy Conversion.

[3] Townsend, T. U. 1989. "A Method for Estimating the Long-Term Performance of Direct-Coupled Photovoltaic Systems." MS Thesis. doi:10.1016/0038-092X(84)90010-0.

[4] Eckstein, J. 1990. "Detailed Modelling of Photovoltaic System Components." MS Thesis.

[5] Schroder, D. K. 2006. Material and Device Semiconductor Material and Device. 3rd ed. Physics Today. doi:10.1063/1.2810086.

[6] Azzouzi, M., Popescu, D., and Bouchahdane, M. 2016. "Modeling of Electrical Characteristics of Photovoltaic Cell Considering Single-Diode Model." Journal of Clean Energy Technologies 4 (6): 414-20. doi:10.18178/JOCET.2016.4.6.323.

[7] Bikaneria, J., Prakash Joshi, S., and Joshi, A. 2013. "Modeling and Simulation of PV Cell Using One-Diode Model." International Journal of Scientific and Research Publications 3 (10): 2250-3153.

[8] Muralidharan, R. 2014. "Mathematical Modeling, Simulation and Validation of Photovoltaic Cells." International Journal of Research in Engineering and Technology 3 (10): 170-4.

[9] Ghosh, S., Shawon, M., Rahman, A., and Abdullah, R. 2013. "Modeling of PV Array and Analysis of Different Parameters." International Journal of Advancements in Research & Technology 2 (5): 358-63.

[10] Elias, B. H., AlSadoon, S. H. M., and Abdulgafar, S. A. 2014. "Modeling and Simulation of Photovoltaic Module Considering an Ideal Solar Cell." International Journal of Advanced Research in Physical Science 1 (August): 9-18.

[11] Petkov, M., Markova, D., and Platikanov, S. 2011. "Modelling of Electrical Characteristics of Photovoltaic Power Supply Sources." *Renew. Energy Sources* 2 (2): 171-7.

[12] Anku, N. E. L., Kankam, A., Takyi, A., and Amponsah, R. 2015. "A Model for Photovoltaic Module Optimisation." Journal of Mechanical Engineering and Automation 5 (2): 72-9. doi:10.5923/j.jmea.20150502.02.

[13] Patel, J., and Sharma, G. 2013. "Modeling and Simulation of Solar Photovoltaic Module Using Matlab/Simulink."

International Journal of Research in Engineering Technology 2 (3): 225-8.

[14] Fares, M. A., Atik, L., Bachir, G., and Aillerie, M. 2017. "Photovoltaic Panels Characterization and Experimental Testing." Energy Procedia 119 (July): 945-52. doi:10.1016/j.egypro.2017.07.127.

[15] Xiao, W., Dunford, W. G., and Capel, A. 2004. "A Novel Modeling Method for Photovoltaic Cells." In *PESC Record—IEEE Annual Power Electronics Specialists Conference*, 3: 1950-6.

[16] Chan, D. S. H., Phillips, J. R., and Phang, J. C. H. 1986. "A Comparative Study of Extraction Methods for Solar Cell Model Parameters." Solid-State Electronics 29 (3): 329-37. doi:10.1016/0038-1101(86)90212-1.

[17] Bellia, H., Youcef, R., and Fatima, M. 2014. "A Detailed Modeling of Photovoltaic Module Using MATLAB." NRIAG Journal of Astronomy and Geophysics 3 (1): 53-61. doi:10.1016/j.nrjag.2014.04.001.

[18] Kittel, C. 2005. Introduction to Solid State Physics, 8th ed. New York: John Wiley.

[19] Ahmad, T., Sobhan, S., and Nayan, F. 2016. "Comparative Analysis between Single Diode and Double Diode Model of PV Cell: Concentrate Different Parameters Effect on Its Efficiency." Journal of Power and Energy Engineering 4 (3): 31-46. doi:10.4236/jpee.2016.43004.

[20] Tsai, H., Tu, C., and Su, Y. 2008. "Development of Generalized Photovoltaic Model Using MATLAB/SIMULINK." Proceedings of the World Congress on Engineering and Computer Science 2008 (WCECS 2008), October 22-24, 2008, San Francisco, USA.

[21] Löper, P., Pysch, D., Richter, A., Hermle, M., Janz, S., Zacharias, M., and Glunz, S. W. 2012. "Analysis of the Temperature Dependence of the Open-Circuit Voltage." Energy Procedia 27: 135-42. doi:10.1016/j.egypro.2012.07.041.